Contribution No. 5023 from the Central Research & Development Department, E. I. du Pont de Nemours & Company, Experimental Station, P.O. Box 80328, Wilmington, Delaware 19880-0328

Electronic Structures of $[Xe_2F_3]^+$ and $XeIF_3$. Examples of 5c,6e Hypervalent Bonding

David A. Dixon,* Anthony J. Arduengo, III, and William B. Farnham

Received February 24, 1989

The electronic structures of known $[Xe_2F_3]^+$ and unknown $[XeIF_3]$ have been calculated by using ab initio molecular orbital theory with polarized, split-valence basis sets. Geometries were gradient optimized, and force fields were calculated. Both molecules are linear. Calculations on IF and XeF_2 were also done to aid in the analysis of the results for $XeIF_3$. The calculated and experimental structures for $[Xe_2F_3]^+$ differ in that the experimental structure is bent at the central fluorine F_c and the Xe–F_c bond distances are calculated to be 0.09 Å too long. The calculated vibrational frequencies for $[Xe_2F_3]^+$ are in reasonable agreement with the experimental values after scaling. The geometry and frequencies for $XeIF_3$ show that the molecule consists of interacting IF and XeF_2 fragments. The minimum dissociation energy of $XeIF_3$ with respect to the two fragments is 17 kcal/mol. The bonding is analyzed in terms of the canonical molecular orbitals and in terms of localized molecular orbitals determined by the Boys criteria. The σ bonding in $[Xe_2F_3]^+$ is a good example of a hypervalent 5c,6e bond. For $XeIF_3$, the interaction is smaller and the bonding is not as delocalized although the components of the 5c,6e hypervalent bond are still present. This is clearly demonstrated by the unequal contributions of the XeF_2 and IF fragments to the various σ orbitals.

Introduction

We have recently extended the concept of the 3c,4e hypervalent bond[1] found in a wide range of molecules to the 5c,6e hypervalent bond.[2] Structures of the form $[R_f\text{–}I\text{–}F\text{–}I\text{–}R_f]^-$ recently prepared in these laboratories[2] are best described in terms of 5c,6e hypervalent bonds. Ab initio molecular orbital theory was used to study the bonding in such complexes with R_f = F and CF_3 and led to the identification of this new type of hypervalent bond. With R_f = F, the anion is isoelectronic and isostructural to the well-known cation $[FXeFXeF]^+$ (**1**),[3] and we present herein a theoretical study of the electronic structure and bonding in this cation. We also present studies on the isoelectronic, isostructural neutral species FXeFIF (**2**).

Although there is much precedent for other $[X_lY_mZ_n]^-$ ions for $l + n + m = 5$, and X = I, and Y, Z = other halogens,[4] the central atom is (or is believed to be) the I, the least electronegative element, in contrast to $[I_2F(R_f)_2]^-$ where the central atom is the F. Furthermore, the well-known structure of I_5^- has a bond angle at the central I of 94°, which is clearly different from our calculated and observed results for $[I_2F(R_f)_2]^-$ ions, which are nearly linear or linear. Thus the bonding in compounds such as I_5^- is clearly distinct from the (5c,6e) examples discussed here.

A simple model for the bonding σ orbitals of the 5c,6e bond based on p orbitals is shown in Chart I. We do not include s or d orbitals or differences in electronegativity in this schematic representation. The S and A labels refer to whether the molecular orbital is symmetric or antisymmetric with respect to a plane perpendicular to the molecular axis and passing through the central atom. The nodal properties are such that the nodes occur at atoms. Thus, in the 5c,6e hypervalent bond just as in the 3c,4e hypervalent bond, there are no nodes between adjacent p orbitals in the occupied σ orbitals. Further analysis of the bonding orbitals shows that the central atom and the terminal atoms have the highest densities and should be the most electronegative. The atoms at positions 2 and 4 should be the least electronegative. This is in contrast to the 3c,4e hypervalent bond where the central atom has the lowest electronegativity and the terminal atoms are the most electronegative. With small modifications to include s and d orbitals, this simple model provides a good description of the bonding in $[FIFIF]^-$.

Chart I

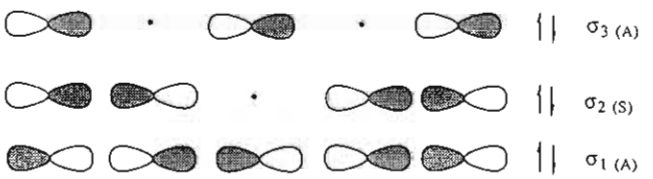

Table I. Geometry Parameters for $[Xe_2F_3]^+$ and $XeIF_3$

param	calc	expt
	$[Xe_2F_2]^+$	
$r(F_T\text{–}Xe)$, Å	1.899	1.90 ± 0.03[a]
$r(F_c\text{–}Xe)$, Å	2.228	2.13 ± 0.03[a]
$\theta(Xe\text{–}F_c\text{–}Xe)$, deg	180	151 ± 2[a]
$\theta(F_T\text{–}Xe\text{–}F_c)$, deg	180	178 ± 2[a]
	$XeIF_3$	
$r(F_T\text{–}Xe)$, Å	1.954	
$r(F_c\text{–}Xe)$, Å	2.014	
$r(F_T\text{–}I)$, Å	1.927	
$r(F_c\text{–}I)$, Å	2.733	
$\theta(Xe\text{–}F_c\text{–}I)$, deg	180	
$\theta(F_T\text{–}Xe\text{–}F_c)$, deg	180	
$\theta(F_T\text{–}I\text{–}F_c)$, deg	180	
	IF	
r(I–F), Å	1.917	1.910[b]
	XeF^+	
r(Xe–F), Å	1.877	
	XeF_2	
r(Xe–F), Å	1.978	1.977[c]
θ(F–Xe–F), deg	180	180[c]
	IF_2^-	
r(I–F), Å	2.077	
θ(F–I–F), deg	180	

[a] Reference 3. [b] Reference 12. [c] Reference 13.

Calculations

Ab initio molecular orbital calculations involving all electrons were performed on **1** and **2** by using the program GRADSCF[5] on a CRAY X-MP/24 computer system. Geometries were gradient optimized.[6] The fluorine basis set was of polarized double-ζ quality with coefficients from Dunning and Hay.[7] The basis set for the central fluorine, F_c, was aug-

(1) (a) Musher, J. I. *Angew. Chem., Int. Ed. Engl.* **1969**, *8*, 54. Musher describes the hypervalent 3c,4e bond in a valence bond formalism based on the models of Pimentel (Pimentel, G. C. *J. Chem. Phys.* **1951**, *19*, 446) and Rundle (Rundle, R. E. *Surv. Prog. Chem.* **1963**, *1*, 81). (b) Cahill, P. A.; Dykstra, C. E.; Martin, J. C. *J. Am. Chem. Soc.* **1985**, *107*, 6359. These authors describe the hypervalent 3c,4e bond in simple molecular orbital terms.

(2) Farnham, W. B.; Dixon, D. A.; Calabrese, J. C. *J. Am. Chem. Soc.* **1988**, *110*, 8453.

(3) (a) Sladky, F. O.; Bulliner, P. A.; Bartlett, N.; DeBoer, B. G.; Zalkin, A. *Chem. Commun.* **1968**, 1048. (b) Bartlett, N.; DeBoer, B. G.; Hollander, F. J.; Sladky, F. O.; Templeton, D. H.; Zalkin, A. *Inorg. Chem.* **1974**, *13*, 780.

(4) Cotton, F. A.; Wilkinson, G. *Advanced Inorganic Chemistry*, 5th ed.; John Wiley & Sons: New York, 1988: (a) pp 577–580; (b) pp 590–591.

(5) GRADSCF is an ab initio gradient program system designed and written by A. Komornicki at Polyatomics Research.

(6) (a) Komornicki, A.; Ishida, K.; Morokuma, K.; Ditchfield, R.; Conrad, M. *Chem. Phys. Lett.* **1977**, *45*, 595. McIver, J. W., Jr.; Komornicki, A. *Chem. Phys. Lett.* **1971**, *10*, 303. (b) Pulay, P. In *Applications of Electronic Structure Theory*; Schaefer, H. F., III, Ed.; Plenum Press: New York, 1977; p 153.

0020-1669/89/1328-4589$01.50/0

Table II. Vibration Frequencies (cm^{-1}) and Intensities (km/mol) for $[Xe_2F_3]^+$ and $XeIF_3$

sym	ν(calc)	ν(expt)	scale	I	assgnt
			$[Xe_2F_3]^+$		
σ_g	704	598[a]	0.849	0	$Xe-F_T$ str
	137			0	$Xe-F_c-Xe$ str
σ_u	696	588[a]	0.845	130	$Xe-F_T$ str
	395			883	$Xe-F_c-Xe$ str
π_g	234	255[a]		60	↑.↑.↑ bend
	51			0.2	↓.↑.↓ bend
π_u	161	161, 171[a]		0	↓....↑ bend
			I–F		
σ	677	610[b]	0.901	59	I–F str
			$Xe-F^+$		
σ	714			4	Xe–F str
			XeF_2		
σ_g	599	557[c]	0.860	0	Xe–F str
σ_u	615	515[c]	0.906	348	Xe–F str
π	248	213[c]	0.858	27	F–Xe–F bend
			$[IF_2]^-$		
σ_g	492			0	I–F str
σ_u	455			391	I–F str
π	219			55	F–I–F bend
			$XeIF_3$		
σ	666	600[d]	0.901	38	$I-F_T$ str
	632	573[e]	0.906	186	$Xe-F_T$ str
	542	466[e]	0.860	474	$Xe-F_c$ str
	63			3	$(F_TXeF_c)-(IF_T)$ str
π	247	212[e]	0.858	52	F_T–Xe–F_c bend
	103			5	F–Xe–F–I–F bend
	21			1.4	F–Xe–F–I–F bend

[a] Reference 18. [b] Reference 14. [c] Reference 20. [d] Scaled by IF scale factor. [e] Scaled by XeF_2 scale factor.

mented with a set of diffuse s (α_s = 0.096) and p functions[7] on the possibility that it has some anion character. The iodine and xenon basis sets are from Huzinaga and co-workers[8] and are split-valence basis sets augmented by a set of valence of polarization functions (α_d = 0.266). The final basis set has the form (16s13p8d/10s6p1d/9s5p1d)/[6s5p3d/4s3p1d/3s2p1d] in the order I, Xe/F_c/F_T. The force fields were determined by using analytic second derivatives, and infrared intensities were also calculated.[9] Correlation corrections were determined at the MP-2 level[10] for the valence electrons. Subsequent analysis of the wave function and the calculation of localized molecular orbitals by the Boys criteria[11] was done by using the program GAMESS,[12] again on the CRAY X-MP/24 computer.

Table III. Total Energies

molecule	angle,[a] deg	basis set[b]	E(SCF), au	E(MP-2), au
$[Xe_2F_3]^+$	180	DZP + diff	−14 751.790 907	−14 752.533 673
$[Xe_2F_3]^+$	170	DZP + diff	−14 751.790 587	−14 752.533 495
$[Xe_2F_3]^+$	160	DZP + diff	−14 751.789 660	−14 752.532 986
$[Xe_2F_3]^+$	150	DZP + diff	−14 751.788 134	−14 752.532 142
$[Xe_2F_3]^+$	180	DZP	−14 751.787 453	−14 752.526 112
$XeIF_3$	180	DZP + diff	−14 438.231 262	−14 438.971 361
$XeIF_3$	180	DZP	−14 438.227 182	−14 438.962 603
XeF_2	180	DZP	−7 425.754 033	−7 426.220 306
$[IF_2]^-$	180	DZP	−7 111.997 679	−7 112.456 820
IF		DZP	−7 012.463 397	−7 012.730 531
$[XeF]^+$		DZP	−7 325.974 129	−7 326.241 670

[a] Bond angle at central atom. [b] DZP + diff is the DZP basis set augmented by diffuse functions on F_c.

Results

Geometries. The geometry parameters are given in Table I, the predicted vibrational spectra are given in Table II, and the total energies are given in Table III. For $[Xe_2F_3]^+$, the crystal structure has been determined by X-ray diffraction methods.[3] There is presently no structure for $XeIF_3$. For $[Xe_2F_3]^+$, the calculated Xe–F_T bond length is in excellent agreement with the experimental value whereas r(F_c–Xe) is calculated to be 0.09 Å too long. The molecule is calculated to have $D_{\infty h}$ symmetry as shown by the force-field calculations described below. The calculated angle for θ(F_c–Xe–F_T) of 180° is in excellent agreement with the observed angle of 178 ± 2°. The calculated angle at the central fluorine θ(I–F_c–I) differs from the observed angle by ~30°. However, as described below, the bending frequency for this angle is very low, 51 cm^{-1}, and various crystal forces due to ionic interactions could easily bend the angle since the potential energy surface is so flat.[13]

In order to confirm the low energy required for bending, SCF and MP-2 calculations (Table III) were done at bond angles of 170, 160, and 150° without varying the bond distance. These results show that the molecule is linear at the MP-2 level and confirm our comment on the flatness of the potential energy surface. At 30° of bend, the energy is only 0.96 kcal/mol higher at the MP-2 level (1.74 kcal/mol higher at the SCF level). Of course, this does not consider any relaxation of other parameters and will be an upper limit. A more detailed examination of the crystal packing shows that the "cations ... generate a three-dimensional network within the cavities of which the AsF_6^- ions are held."[3b] Indeed F_c interacts most closely with two F_T's (r ~ 3.0 Å) from different $[Xe_2F_3]^+$ ions. Combining these close interactions with the need for linear species to pack around a spherical counterion, it is not surprising to see a difference between the calculated and observed structures.

The calculated structure for $[Xe_2F_3]^+$ can also be compared to that of $[I_2F_3]^-$, both of which have $D_{\infty h}$ symmetry. The I–F_c bond is 0.05 Å longer than the Xe–F_c bond and the Xe–F_T bonds are 0.094 Å shorter than the I–F_T bonds just as found in comparing $[IF_2]^-$ and XeF_2 and IF and $[XeF]^+$; vide infra.

The molecule FXeFIF has unequal Xe–F_c and I–F_c bond distances with r(Xe–F_c) much shorter than r(I–F_c). Thus the molecule resembles an IF strongly interacting with XeF_2. In order to calibrate our results, we calculated the geometries of IF and XeF_2. The calculated and experimental values[14] for IF are in excellent agreement. The calculated value for r(Xe–F) for XeF_2 is also in excellent agreement with the experimental gas-phase value.[15] The I–F_T bond distance of 1.927 Å is only 0.010 Å longer

(7) Dunning, T. H., Jr.; Hay,P. J. In *Methods of Electronic Structure Theory*; Schaefer, H. F., III, Ed.; Plenum Press: New York, 1977; p 1.

(8) *Gaussian Basis Sets for Molecular Calculations* Huzinaga, S., Ed.; Physical Sciences Data 16; Elsevier: Amsterdam, 1984.

(9) (a) King, H. F.; Komornicki, A. In *Geometrical Derivatives of Energy Surfaces and Molecular Properties*; Jorgenson, P., Simons, J., Ed.; NATO ASI Series C 166; D. Reidel: Dordrecht, The Netherlands, 1986; p 207. (b) King, H. F.; Komornicki, A. *J. Chem. Phys.* **1986**, *84*, 5645.

(10) (a) Moller, C.; Plesset, M. S. *Phys. Rev.* **1934**, *46*, 618. (b) Pople, J. A.; Binkley, J. S.; Seeger, R. *Int. J. Quantum Chem., Symp.* **1976**, *10*, 1.

(11) (a) Boys, S. F. In *Quantum Theory of Atoms, Molecules and the Solid State*; Löwdin, P.-O., Ed.; Academic Press: New York, 1966; p 253. (b) Kleier, D. A.; Halgren, T. A.; Hall, J. H., Jr.; Lipscomb, W. N. *J. Chem. Phys.* **1974**, *61*, 3905.

(12) GAMESS program system from M. Schmidt, North Dakota State University, and S. Elbert, Iowa State University, based on the original program from NRCC: Dupuis, M.; Spangler, D.; Wendoloski, J. J. *National Resource for Computation in Chemistry Software Catalog*; Lawrence Berkeley Laboratory, USDOE: Berkeley, CA, 1980; Vol. 1, program QG01. See also: Dupuis, M.; Rys, J.; King, H. F. *J. Chem. Phys.* **1976**, *65*, 111.

(13) There are a number of recent studies on very flat potential energy surfaces where the question of correlation effects on bond angles have been raised. For example, see the discussion on CF_3CSF_3 in: Dixon, D. A.; Smart, B. E. *J. Am. Chem. Soc.* **1986**, *108*, 2688. Christen, D.; Mack, H.-G.; Marsden, C. J.; Oberhammer, H.; Schatte, G.; Seppelt, K.; Willner, H. *J. Am. Chem. Soc.* **1987**, *109*, 4009.

(14) Huber, K. P.; Herzberg, G. *Constants of Diatomic Molecules*; van Nostrand-Reinhold: New York, 1979.

(15) Reichman, S.; Schreiner, F. *J. Chem. Phys.* **1969**, *51*, 2355. See ref 16 for the solid-state structure and ref 17 for other theoretical work.

than the calculated distance of diatomic IF where r(I–F) = 1.917 Å. The Xe–F_T bond distance is 0.024 Å shorter than the calculated value of r(Xe–F) = 1.978 Å in XeF_2 and the calculated value for XeF_c of 2.014 Å is 0.036 Å longer than that calculated for XeF_2. The value for r(I–F_c) of 2.733 is 0.72 Å longer than the value for r(Xe–F_c). The calculated structure of $XeIF_3$ differs from that found for other XeF_2 Lewis acid complexes. In these latter cases, the XeF_2 transfers F^- to the Lewis acid to form complexes such as $2XeF_2 \cdot SbF_5$, $XeF_2 \cdot AsF_5$, and $XeF_2 \cdot 2RuF_5$ where the species containing the Xe is a cation.[4b] In our case, the F^- is not transferred because IF is not a strong enough F^- acceptor leading to strongly interacting neutral molecules.

For completeness, we calculated the structures of the ions $[XeF]^+$ and $[IF_2]^-$, which are isoelectronic with IF and XeF_2. The Xe–F bond length in $[XeF]^+$ is slightly shorter than the I–F bond length in IF but is 0.1 Å shorter than the Xe–F bond in XeF_2. The ion $[IF_2]^-$ has $D_{\infty h}$ symmetry as found for XeF_2, and as would be expected, the I–F bond distance is 0.1 Å longer in $[IF_2]^-$ in comparison with the Xe–F bond in XeF_2.

Frequencies. The calculated vibrational spectra for $[Xe_2F_3]^+$ and $XeIF_3$ are shown in Table II. The symmetric and asymmetric XeF_T stretches in $[Xe_2F_3]^+$ are split by less than 10 cm^{-1} and are much higher frequency than the stretches involving the xenons and F_c. These latter stretches show a large splitting with the asymmetric stretch near 400 cm^{-1} and the symmetric stretch near 140 cm^{-1}. We predict that the σ_u band calculated near 400 cm^{-1} should be very intense. The bends are calculated at 234, 137, and 51 cm^{-1}. As discussed above, the very low bending frequency of 51 cm^{-1} means that the molecule could easily be bent in the crystal by ionic forces and can account for the difference between the calculated and experimental Xe–F_c–Xe bond angles.

There are experimental Raman measurements[3a,18] available for the $[Xe_2F_3]^+[AsF_6]^-$ and $[Xe_2Fe_3]^+[SbF_6]^-$ salts, and we can compare our results with these values. The agreement between the calculated and experimental values is not exact for a number of reasons. First, we have neglected correlation corrections and we have calculated harmonic frequencies rather than the observed anharmonic values. These differences can usually be accounted for by appropriately scaling the calculated frequencies.[19] Typical scale factors for first-row compounds are 0.9, but scale factors as low as 0.85 are often found for molecules with heavier elements. Second, the molecular structure in the solid state is bent, most likely due to the presence of the anions, and some differences are expected (for example, our calculated results show a rigorous exclusion rule for IR and Raman bands). For the two highest frequency stretches (involving Xe–F_T), we find scale factors of ~0.85. The calculated splitting of 8 cm^{-1} for these stretches is in good agreement with the experimental value of 10 cm^{-1}.[18] The σ_u mode for the Xe–F_c–Xe asymmetric stretch is calculated at 395 cm^{-1}. A very weak Raman band is observed between 400 and 420 cm^{-1}.[18] Since the molecule is only slightly bent in the crystal and this band is not Raman-allowed for the linear structure, the Raman intensity should be weak. It is somewhat surprising that the calculated frequency is below the experimental value. This could easily be due to the fact that the experimental ion is bent whereas the calculated structure is linear and a shift of 30–50 cm^{-1} could be expected. A reasonably intense Raman band near 160 cm^{-1} is also observed,[3a,18] and we assign this band as the π_u bend, which we calculate at 161 cm^{-1}. In $[Xe_2F_3]^+[SbF_6]^-$, two bands are clearly observed at 161 and 171 cm^{-1} with a probable shoulder at 179 cm^{-1}. The two bands at 161 and 171 cm^{-1} are the two components of our calculated π_u bond that is split by bending in the crystal. A weak, broad band is observed at 255 cm^{-1}. This is the π_g bend that we calculate at 234 cm^{-1}. The fact that the observed frequencies are above the calculated ones is again probably due to the difference in bond angles. The calculated bands at 137 and 51 cm^{-1} are not observed experimentally, the latter due to the width of the Raman exciting line.

Table IV. Orbital Energies for $[Xe_2F_3]^+$ and $XeIF_3$

$[Xe_2F_3]^+$			$XeIF_3$		
sym	descrpn	ϵ, eV	sym	descrpn	ϵ, eV
π_g	Xe LP	18.67	π	I LP	10.35
π_u	Xe LP	19.04	π	Xe LP (deloc)	14.51
σ_u	σ_3	20.18	σ	σ_4	15.30
π_g	F_c LP	22.66	σ	σ_3	16.53
σ_g	σ_2	23.10	π	F_T(I) LP	17.34
π_u	F_T LP	23.83	π	F_T(Xe) + α-F_c LP	18.20
π_g	F_T LP	23.88	π	F_c + α-F_T(Xe) + β-Xe LP	18.97
σ_u	σ_1	25.50	σ	σ_2	20.61
			σ	σ_1	23.16

The vibrational spectrum for $XeIF_3$ is also shown in Table II. We first compare our calculated spectra for XeF_2 and IF with the experimental values. For IF, a scale factor of 0.90 is needed.[14] For XeF_2,[20] scale factors of 0.91 are needed for the σ_u stretch and 0.86 for the σ_g stretch and the π bend. The calculated splitting of the asymmetric and symmetric stretches is somewhat smaller than the observed splitting. The calculated spectral data for $[XeF]^+$ and $[IF_2]^-$ are also given in Table II. As expected from the bond distances, the Xe–F stretch in $[XeF]^+$ is larger than the I–F stretch in IF. The frequencies in $[IF_2]^-$ are smaller than those in XeF_2 in a similar fashion. The σ_g and σ_u stretches have a different ordering in $[IF_2]^-$ than in XeF_2.

As discussed previously, the structure for $XeIF_3$ shows distinct IF and XeF_2 fragments. The calculated vibrational frequencies show similar behavior. The IF frequency is red-shifted by 10 cm^{-1} in the complex. The XeF_2 frequencies are split further apart in the complex. The Xe–F_T stretch increases by 17 cm^{-1} from the asymmetric stretch value in XeF_2 whereas the Xe–F_c stretch decreases by 55 cm^{-1} in the complex when compared to the symmetric stretch in XeF_2. These results are consistent with the decrease in r(Xe–F_T) and the increase in r(Xe–F_c) when compared to XeF_2. The XeF_2 bend is the same in the complex as in free XeF_2. The remaining bends are significantly lower in frequency with the lowest bend at 21 cm^{-1}. The lowest energy stretch at 63 cm^{-1} corresponds to dissociation of the complex and clearly demonstrates that $XeIF_3$ is a bound species. However, it is expected to be very floppy.

The dissociation energy of $XeIF_3$ into XeF_2 and IF can be calculated from the total energies. The energy for $XeIF_3$ was recalculated after the diffuse functions on F_c were dropped in order to have the same basis set for reactants and products. The binding energy of $XeIF_3$ is 6.1 kcal/mol at the SCF level and 7.4 kcal/mol at the MP-2 level. Although this is not a large binding energy, it is significantly greater than the expected van der Waals energy; e.g., for $(I_2)_2$, the binding energy is 1.1 kcal/mol from viscosity data,[21] consistent with the formation of a very weak chemical bond in $XeIF_3$. For comparison, the binding energy of $[Xe_2F_3]^+$ into XeF_2 and $[XeF]^+$ is much larger, 40.2 kcal/mol at the MP-2 level (37.2 kcal/mol at the SCF level), consistent with the formation of an equally distributed 5c,6e bond.

MO Bonding Analysis. We analyzed the bonding in $[Xe_2F_3]^+$ as we previously analyzed the bonding in $[I_2F_3]^-$.[2] The orbital energies and descriptions are shown in Table IV and the orbital diagrams are shown in Figure 1. The HOMO and NHOMO are each degenerate and are the lone pairs on the xenons. The first σ orbital is predominantly of p type character with the fluorine orbitals having the largest density. The largest density is on the central fluorine with about half of that density on the terminal fluorines. The small s orbital component on the Xe's is out-of-phase with the p orbitals, but the small d-orbital component has

(16) Levy, H. A.; Agron, P. A. *J. Am. Chem. Soc.* **1963**, *85*, 241.
(17) (a) Bagus, P. S.; Liu, B.; Liskow, D. H.; Schaefer, H. F., III. *J. Am. Chem. Soc.* **1975**, *97*, 7216. (b) Bartell, L. S.; Rothman, M. J.; Ewig, C. S.; Van Wazer, J. R. *J. Chem. Phys.* **1980**, *73*, 367.
(18) Gillespie, R. J.; Landa, B. *Inorg. Chem.* **1973**, *12*, 1383.
(19) Dixon, D. A. *J. Phys. Chem.* **1988**, *92*, 86.
(20) (a) Smith, D. F. *J. Chem. Phys.* **1963**, *38*, 270. (b) Tsao, P.; Cobb, C. C.; Claassen, H. H. *J. Chem. Phys.* **1971**, *54*, 5247. (c) Ault, B. S.; Andrews, L.; Green, D. W.; Reedy, G. T. *J. Chem. Phys.* **1977**, *66*, 2786.
(21) Hirschfelder, J. O.; Curtiss, C. F.; Bird, R. B. *Molecular Theory of Gases and Liquids*; John Wiley & Sons: New York, 1954; pp 1110–1113.

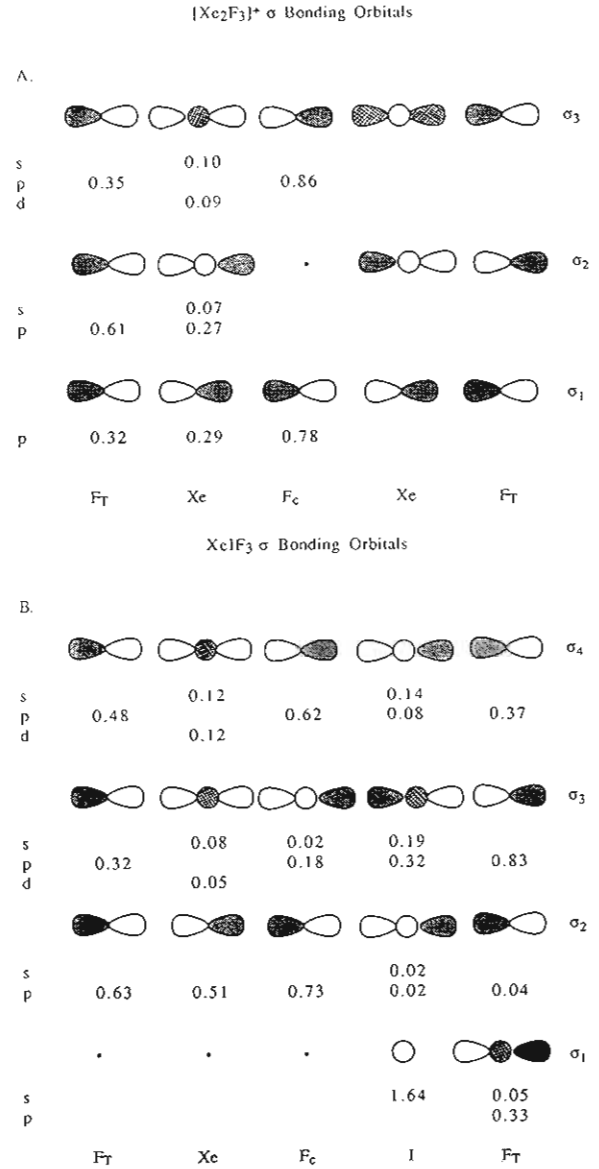

Figure 1. Schematics of the occupied σ orbitals for the 5c,6e hypervalent bonds in $[Xe_2F_3]^+$ (A) and $XeIF_3$ (B). The populations directly beneath each atomic orbital are the total Mulliken charges for that AO in the specific MO in units of electrons. The populations are labeled s, p, and d.

a bonding interaction. Thus, there is less nodal character in $Xe_2F_3^+$ in the σ HOMO than would be expected based on the all-p-orbital model for a 5c,6e bond. The next two orbitals (π_g orbital) are the lone pairs on F_c. The next σ orbital has a node at the central atom and, as would be expected, has bonding interactions between the Xe and F_T. The dominant density here is found on the electronegative terminal fluorines. The next four orbitals are the π_u and π_g orbitals, which are the lone pairs on the terminal fluorines. The final important bonding σ orbital for the 5c,6e bond has no nodes. The largest density is on the central fluorine, and the Xe and F_T have comparable densities. The sum of the populations on each F_T and Xe pair is 0.61e, 0.17e less than the population on F_c. Thus the σ bonding is exactly that expected for the 5c,6e bond and follows the model that we developed for $[I_2F_3]^-$.

Since there is no center of symmetry in $XeIF_3$, the bonding differs somewhat from that found for $[Xe_2F_3]^+$. The HOMO and NHOMO are π orbitals and are predominantly the lone pairs on I and Xe, respectively. There is some delocalization of these lone pairs onto the adjacent fluorines. For I, the delocalization is to its adjacent F_T whereas, for Xe, the delocalization is to the adjacent F_T and to F_c. The highest σ orbital is clearly delocalized. The largest population is on F_c followed by the F_T bonded to Xe. There is also a significant population on the F_T bonded to I. The Xe and I both have reasonable populations, 0.24e on Xe and 0.22e on I. The contributing orbitals on Xe are the s and d orbitals expected from the $[Xe_2F_3]^+$ results whereas, for I, the s and p orbitals contribute. The next σ orbital has its largest component on the F_T bonded to I with the next largest population, 0.51e, on the I. Although this orbital is clearly dominated by an I–F σ bond there is a substantial population of 0.32e on the other F_T. Because there is no center of symmetry, F_c can contribute to the bond and has a population of 0.18e. The next six orbitals are the fluorine lone pairs. The least stable lone pair is on the F_T bonded to I, followed by a delocalized lone pair with its largest population on F_c and finally by another delocalized lone pair with its largest population on F_T bonded to Xe. The lowest σ orbital in the five-center hypervalent bond has very little population on the I–F_T fragment and is most like the lowest energy XeF_2 bonding σ orbital. The p orbital on the F_T bonded to I mixes significantly with the I valence "s" orbital rather than contributing to the 5c,6e bond.

Table V. Mulliken Charges

atom	q, e	atom	q, e
	$[Xe_2F_3^+]$		
F_c	−0.62	Xe	1.16
F_T	−0.35		
	XeF_2		
F	−0.53	Xe	1.06
	$[IF_2]^-$		
F	−0.69	I	0.37
	$XeIF_3$		
F_T(I)	−0.50	Xe	1.03
F_c	−0.52	I	0.47
F_T(Xe)	−0.48		
	IF		
F	−0.44	I	0.44
	$[XeF]^+$		
F	−0.23	Xe	1.23

The Mulliken charges are given in Table V. The charges for $[Xe_2F_3]^+$ show the Xe's to be quite positive and the F's to be negative. The most negative fluorine is F_c with the negative charges on F_T being about half of this value. The xenons are expected to be quite positive because even in neutral XeF_2 the Xe has a charge of 1.06e. The Xe–F_T fragments each have charges of 0.81e and F_c balances these positive charges with a charge of −0.62e. However, there is clearly not a full negative charge on F_c, and the molecule is not completely described as two $[XeF]^+$ fragments held by an F^-; there is clearly a covalent component consistent with the 5c,6e hypervalent bond.

For $XeIF_3$, we can compare the charges with those of the isolated fragments XeF_2 and IF. The I becomes more positive in the complex and the F_T(I) becomes more negative as compared to diatomic IF. There is a net negative charge of 0.03e on the IF fragment. The XeF_2 fragment is thus slightly positive. The electron density transferred from the XeF_2 fragment to the IF fragment comes from the fluorines. The Xe is actually less positive in the complex than in the triatomic moiety. The fluorines are less negative in the complex with F_c losing the most density. These results are consistent with weak hypervalent bonding in $XeIF_3$.

LMO Bonding Analysis. Another technique for examining the bonding in molecules is to examine the localized molecular orbitals generated by an appropriate transformation of the wave function.[22] This unitary transformation, of course, leaves the total energy and density invariant. Only the valence orbitals were localized by following the Boys criteria. The orbital centroids are given in the supplementary material together with the molecular coordinates. As discussed below, the localization for **1** converged very slowly. The orbitals (shown schematically in Chart II) clearly show three

(22) Lipscomb, W. N. *Acc. Chem. Res.* **1973**, *6*, 257.

Chart II

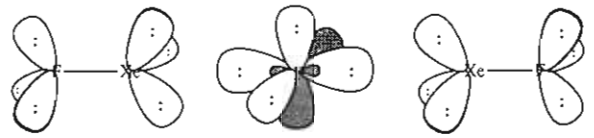

Chart III

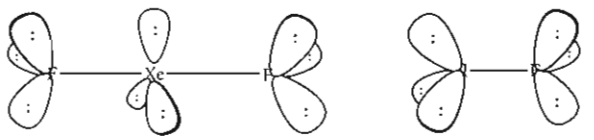

lone pairs on each of the terminal fluorines that are bent away from the σ bond and the Xe. There are three lone pairs on each Xe bent away from the σ bond and F_T toward F_c. There are two Xe–F_T σ bonds that have centroids closer to the F_T than to Xe. The remaining four valence orbitals are predominantly on F_c. There are two lone pairs that are $sp^{3.5}$ hybrids approximately perpendicular to each other and to the molecular axis. The remaining two orbitals are similar to lone pairs on F_c that are delocalized onto the xenons by 0.10–0.12e. The orbitals bend away from the molecular axis and have hybridizations of $sp^{2.41}$ and $sp^{2.56}$. The Boys LMO criteria is known to be biased against σ–π (s–p) separation because it tries to have maximum separation of the centroids of charge for each orbital. The 5c,6e hypervalent bond for this system has s–p separation in that the hypervalent bond is composed of p orbitals (σ_2 in Figure 1A has only 0.03e in the 2s on F_c) and does not include the 2s orbital on F_c. Thus, the centroids of charge of the p orbital (on F_c involved in the σ bond) and the 2s orbital are identical. The Boys criteria tries to maximally separate these centroids. However, this is difficult, leading to very poor convergence.

For $XeIF_3$, there are no symmetry constraints as in $[Xe_2F_3]^+$ on σ–π separation and the localization converges quickly. There are three lone pairs on each atom and there are three σ bonds, I–F_T, Xe–F_T and Xe–F_c (Chart III). Thus the LMO's for $XeIF_3$ do not show any of the bonding found in our analysis of the hypervalent 5c,6e bond based on the canonical MO's.

Conclusions

The analysis of the canonical molecular orbitals clearly shows the presence of a 5c,6e hypervalent bond in $[Xe_2F_3]^+$. The atomic charges are also consistent with such a description. The LMO's on the other hand do not show such a description well precisely because they are localized. The hypervalent 5c,6e bond requires delocalization over five centers. Furthermore, there are only three electron pairs to distribute over four bonding interatomic regions. Thus the LMO's converge poorly and prefer a picture more consistent with a fully ionic model, i.e., an F^- binding two $[Xe–F]^+$ fragments. However, the LMO's do try to make weak σ bonds between F_c and the Xe's consistent with the hypervalent model. For $XeIF_3$, the description of the bonding is more complex. The highest occupied σ_4 orbital clearly has a 5c,6e hypervalent bond component as does the σ_3 orbital. However, the bonding σ_2 and σ_1 orbitals are more like those of the fragment molecules XeF_2 and IF, especially with the mixing of the fluorine p with the valence s on iodine as found in σ_1. With this behavior of σ_1 and σ_2 for the canonical molecular orbitals, it is not surprising that the LMO's are essentially those of the isolated fragments. However, the calculated geometry, vibrational spectra, and energetics for $XeIF_3$ are consistent with more than weakly interacting fragments and there is some component of a hypervalent bond.

Registry No. $[Xe_2F_3]^+$, 37366-73-7; $[XeIF_3]$, 123148-33-4; XeF_2, 64054-70-2; IF, 13873-84-2; $[XeF]^+$, 47936-70-9; $[IF_2]^-$, 25730-98-7.

Supplementary Material Available: A table of molecular coordinates and LMO centroids of charge for $[Xe_2F_3]^+$ and $XeIF_3$ (2 pages). Ordering information is given on any current masthead page.

Contribution from the Dipartimento di Scienze Chimiche and Istituto Chimico, Facoltà di Ingegneria, Università di Catania, 95125 Catania, Italy, and Department of Chemistry, Louisiana State University, Baton Rouge, Louisiana 70803-1804

Preparation, Characterization, and Structural Aspects of Transition-Metal Complexes with 4,7,10-Trioxa-1,13-dithia[13](2,5)-1,3,4-thiadiazolophane

Raffaele Bonomo,[†] Francesco Bottino,[†] Frank R. Fronczek,[‡] Antonino Mamo,[§] and Sebastiano Pappalardo*,[†]

Received February 8, 1989

The title compound **5** readily forms discrete 2:1 (ligand to metal) complexes with Cu(II), Co(II), and Ni(II) nitrates and with $CuBr_2$ and a highly crystalline polymeric 2:3 (ligand to metal) complex with $CdCl_2$. The complexes have been characterized by chemical analysis, FAB mass spectrometry, ^1H NMR spectroscopy (for the diamagnetic Cd(II) complex **10**), electronic spectral studies, and EPR spectroscopy. Structures of the free ligand and its complexes with $CuBr_2$ and $CdCl_2$ have also been determined. X-ray crystal structure determinations have shown that the macrocyclic ligand does not accommodate the metal ions inside the cavity but rather coordinates on the exterior through a nitrogen atom(s). The heterocyclic ring acts as a monodentate ligand in the trans square-planar Cu(II) complex **9** and as a bridging bidentate ligand in the octahedral Cd(II) complex **10**. Cd atoms in **10** are linked through bis(μ-chloro) bridges into infinite chains, the macrocyclic units serving as bridging ligands through the two nitrogen atoms. $C_{10}H_{16}N_2O_3S_3$ (**5**) is tetragonal, $P4_12_12$ (or $P4_32_12$), with a = 9.3369 (11) Å, c = 15.761 (2) Å, Z = 4, and R = 0.027 for 1653 observations. $CuBr_2(C_{10}H_{16}N_2O_3S_3)_2$ (**9**) is triclinic, $P\bar{1}$, with a = 8.3452 (13) Å, b = 9.2414 (10) Å, c = 11.7586 (8) Å, α = 71.313 (7)°, β = 78.347 (9)°, γ = 63.120 (12)°, Z = 1, and R = 0.043 for 3033 observations. $Cd_3Cl_6(C_{10}H_{16}N_2O_3S_3)_2{\cdot}2CH_3OH$ (**10**) is triclinic, $P\bar{1}$, with a = 10.133 (3) Å, b = 10.187 (2) Å, c = 11.740 (2) Å, α = 72.834 (11)°, β = 68.327 (15)°, γ = 63.52 (2)°, Z = 1, and R = 0.020 for 3206 observations.

Introduction

Various 1,3,4-thiadiazole sulfur derivatives are well-known for their ability to form stable complexes with heavy- and transition-metal ions.[1] 2,5-Dimercapto-1,3,4-thiadiazole (**1**, Bismuthiol I) is among the most extensively studied ligands of this class[2] and has found application as an analytical reagent in the detection and determination of metal ions,[3] and its complexes have industrial

[†] Dipartimento di Scienze Chimiche, Università di Catania.
[‡] Louisiana State University.
[§] Istituto Chimico, Facoltà di Ingegneria, Università di Catania.

(1) Sandström, J. *Adv. Heterocycl. Chem.* **1968**, *9*, 165.
(2) (a) Gajendragad, M. R.; Agarwala, U. *Aust. J. Chem.* **1975**, *28*, 743. (b) Gajendragad, M. R.; Agarwala, U. *J. Inorg. Nucl. Chem.* **1975**, *37*, 2429. (c) Zaidi, S. A. A.; Farooqi, A. S.; Varshney, D. K.; Islam, V.; Siddiqi, K. S. *J. Inorg. Nucl. Chem.* **1977**, *39*, 581. (d) Osman, M. M.; Makhyoun, M. A.; Tadros, A. B. *Bull. Soc. Chim. Fr.* **1980**, 451.

0020-1669/89/1328-4593$01.50/0